Small-Angle X-ray Solution-Scattering Studies on Ligand-Induced Subunit Interactions of the Thiamine Diphosphate Dependent Enzyme Pyruvate Decarboxylase from Different Organisms†

Stephan König,*,‡ Dmitri I. Svergun,§,⊥ Vladimir V. Volkov,⊥ Lev A. Feigin,⊥ and Michel H. J. Koch§

Fachbereich Biochemie/Biotechnologie, Institut für Biochemie, Martin-Luther-Univerität Halle−Wittenberg, Halle/Saale, Germany, European Molecular Biology Laboratory (EMBL c/o DESY), Hamburg Outstation, Germany, and Institute of Crystallography, Russian Academy of Sciences, Moscow, Russia

Received August 26, 1997; Revised Manuscript Received February 10, 1998

ABSTRACT: The quaternary structures of the thiamine diphosphate dependent enzyme pyruvate decarboxylase (EC 4.1.1.1) from the recombinant wild type of *Saccharomyces cerevisiae* and *Zymomonas mobilis* and from germinating *Pisum sativum* seeds were examined by X-ray solution scattering. The dependence of the subunit association equilibrium on the pH and the presence of the cofactors thiamine diphosphate and magnesium ions were compared, and the differences between the catalytic properties of the different enzymes are discussed. The influence of amino acid substitutions at the cofactor binding site of the enzyme from *Saccharomyces cerevisiae* (E51 is substituted by Q or A and G413 by W) on the subunit association was examined. Low-resolution models of the *P. sativum, Z. mobilis*, and *S. cerevisiae* enzymes were evaluated ab initio from the scattering data. The enzyme from the bacterium and yeast appear as a dimer of dimers, whereas the plant enzyme is an octamer formed by two tetramers arranged side-by-side. The shape of the *S. cerevisiae* enzyme agrees well with the atomic structure in the crystal but suggests that the dimers in the latter should be tilted by approximately 10°. The resulting modification of the atomic structure also yields a significantly better fit to the experimental solution scattering data than that calculated form the original crystallographic model.

Previous X-ray scattering studies on pyruvate decarboxylase (PDC)[1] from brewer's yeast have shown that there is a pH-dependent equilibrium between dimers and tetramers in solution (*1*) and that the rate of dissociation of the cofactors is equal to the rate of reversible enzyme inactivation and proportional to the fraction of dimeric enzyme. Effectors (the activator pyruvamide, the inhibitor inorganic phosphate, and the cofactors thiamine diphosphate and magnesium ions) influence the equilibrium between subunits, but only the cofactors significantly stabilize the tetramers (*2*). The low-resolution structural models of the dimers and tetramers of PDC from brewer's yeast obtained in the course of these studies were later confirmed by the crystal structure of one of the isoforms of the enzyme (*3*, *4*).

All PDCs described so far consist of nearly identical subunits with molecular masses around 60 kDa, and a set of cofactors—one TDP molecule and one divalent metal ion—is bound very tightly but noncovalently at pH 6. The conformation of TDP in the active centers is very similar in all enzymes analyzed so far by X-ray crystallography (*5*) and corresponds to the "V" conformation (*6*) predicted on the basis of comprehensive kinetic studies with a number of coenzyme derivatives (*7*). The dissociation of the cofactors proceeds at alkaline pH values (above 7) and can easily be monitored over the reduction of the catalytic activity, which in turn is linked to a change in the quaternary structure (*8*). The catalytic activity of the enzymes from *Saccharomyces cerevisiae* and from *Pisum sativum* is regulated by their substrate pyruvate (*9*, *10*). The kinetics of this activation results in a sigmoid dependence of the reaction rate on substrate concentration. The expected large conformational changes during enzyme activation were proven by cross-linking experiments with the brewer's yeast enzyme (*11*) and by the crystal structure of the pyruvamide-activated state of this enzyme (*12*). In the activated state of PDC, two of the active sites are closed by flexible loops which are, however, not visible in the crystal structure of the native enzyme (*4*). PDC from *Zymomonas mobilis* is not substrate-regulated. This enzyme has a lower K_M for its substrate pyruvate (0.4 mM (*13*) compared to 1 mM for the activated state of the yeast and plant enzyme, respectively (*9*, *14*)) and higher catalytic activity (180 U/mg compared to 60−80 U/mg for the others). The catalytically active quaternary forms are tetramers in yeast and bacterial PDC and higher oligomers in the enzyme from germinating pea seeds (*14*) as well as in other plant species (*15*); however, there is no precise description of the catalytically active states of plant PDCs.

† This work was partially funded by the Bundesministerium für Bildung, Wissenschaft, Forschung und Technologie (Grants No. 05-641KEB0 and No. 03-K04HAL-2), and by the INTAS (Grants No. 95-1272 and No. 96-1115).

* Corresponding author. Telephone: -345/5524829. Fax: -345/5527011. E-mail: koenig@biochemtech. uni-halle.de.

‡ Martin-Luther-Universität Halle−Wittenberg.

§ European Molecular Biology Laboratory.

⊥ Russian Academy of Sciences.

[1] Abbreviations: PDC, pyruvate decarboxylase; TDP, thiamine diphosphate; DTE, 1,4-dithioerythritol; SAXS, small-angle X-ray solution scattering; PDB, Protein Data Bank.

S0006-2960(97)02125-9 CCC: $15.00
Published on Web 03/24/1998

Small-angle X-ray scattering with synchrotron radiation allows us to make static and dynamic studies of the ligand-induced changes in the interactions between subunits in solution. The effect of the cofactors on subunit association can thus be studied as an independent level in the regulation of enzymatic activity. Low-resolution models of the shape of the enzyme can be computed from precise scattering curves. When the crystal structures are available, these calculations provide a check for the consistency of the crystal and solution structures (*16,17*) and further allow us to analyze the differences in terms of domain movements. Otherwise, as in the case of PDC from *Z. mobilis* and germinating seeds of *P. sativum*, they provide the first direct evidence for the quaternary structure of these enzymes.

MATERIALS AND METHODS

All enzymes were freshly prepared following the methods of Sieber et al. (*18*), modified by König et al. (*1*) for PDC from brewer's yeast, of Killenberg-Jabs et al. (*19*) for recombinant PDC (wild type and mutants G413W, E51A, and E51Q) from *S. cerevisiae* (the strains were kindly provided by I. Eberhardt and S. Hohmann, Instituut voor Plantkunde, Katholieke Universiteit Leuven, Belgium), of Mücke et al. (*14*) modified by Dietrich (unpublished) for PDC from germinating seeds of *P. sativum* cv. Miko as well as of Schäffner (unpublished) for recombinant wild-type PDC from *Z. mobilis*.

Except for samples requiring preincubation, the solutions were prepared immediately before the X-ray scattering measurements from enzyme stock solutions at the highest possible concentrations (8−25 mg/mL). For pH dependence studies, good buffers with pH values corresponding to the pK_a of the buffer substances were used exclusively. Effectors were added at saturating concentrations (10 mM thiamine diphosphate, magnesium sulfate). Possible denaturation of the enzymes during the X-ray scattering measurements could be excluded by reference measurements of the protein absorption and the catalytic activity of the irradiated samples. Measuring temperatures of 7 °C and addition of 1 mM DTE to all sample buffers guaranteed residual activities above 90% of the original ones for all samples (*2*). All protein concentrations and pH values used for parameter calculation were determined with the original samples after the measurements.

The solution scattering data were collected following standard procedures with the X33 camera (*20*−*22*) of the EMBL in HASYLAB on the storage ring DORIS of the Deutsches Elektronen Synchrotron (DESY) at Hamburg using multiwire proportional chambers with delay line readout (*23*). Data were collected at three different camera lengths (1.3, 2.7, and 4 m) covering ranges of momentum transfer $s = 4\pi \sin\theta/\lambda$ (2θ is the scattering angle and $\lambda = 0.15$ nm is the wavelength) between 0.1 and 2.6 nm^{-1}. Bovine serum albumin (Merck) and DNA from calf thymus (Sigma−Aldrich) were used as calibration substances for the calculation of molecular masses and mass/length ratios, respectively. Protein concentrations of 7 mg/mL for the enzyme from *P. sativum*, 3−15 mg/mL for the enzyme from *Z. mobilis*, and 5−24 mg/mL for that from recombinant wild type and mutants of *S. cerevisiae* were used during the measurements. The experimental data were normalized to the intensity of the incident beam and corrected for the detector response, the buffer scattering was subtracted and the statistical errors were calculated using the program Sapoko (Svergun and Koch, unpublished). The data were processed with the program Gnomoko—a version of the indirect transform package Gnom (*24*−*26*) running on an IBM PC—to obtain the forward scattering intensity ($I(0)$) and the radius of gyration (R_G) or the radius of gyration of the cross section (R_x). The molecular masses were calculated from the ratios of $I(0)$ to protein concentrations of bovine serum albumin (or calf thymus DNA) and of the samples. The oligomer contents were calculated using the merged processed files in the program Oligomer (Svergun, unpublished).

For the ab initio shape determination, envelopes of the enzymes were parametrized using spherical harmonics such as (*16, 27*)

$$F(\omega) = \sum_{l=0}^{L} \sum_{m=-l}^{l} f_{lm} Y_{lm}(\omega) \qquad (1)$$

where $\omega = (\theta,\varphi)$ are the spherical coordinates, f_{lm} are complex numbers, Y_{lm} are the spherical harmonics, and the value L defines the resolution of the shape representation which is equal to $\delta r = \pi R_0/(L+1)$, where $R_0 = (5/3)^{1/2} R_G$ is the radius of the equivalent sphere. Higher oligomer structures, e.g., tetramers or octamers, usually display a 222 symmetry (which is also the case for native yeast PDC (*4*)), and this symmetry restriction was used to reduce the number of model parameters. The shape determinations were performed with terms up to $L = 6$, which, assuming 222 symmetry, yields 13 free parameters f_{lm} in expansion 1. The latter were determined with a nonlinear optimization procedure by minimizing the discrepancy (χ^2) between the experimental and calculated ($I(s_j)$) curves

$$\chi^2 = \frac{1}{N-1} \sum_j \left[\frac{I(s_j) - I_{exp}(s_j)}{\sigma(s_j)} \right]^2 \qquad (2)$$

where N is a number of experimental points and $I_{exp}(s)$ and $\sigma(s)$ are the experimental intensity and its standard deviation, respectively. The scattering curves from the atomic models are calculated using the program Crysol (*28*), which surrounds the macromolecule in solution by a hydration layer of a thickness of 0.3 nm with an adjustable density ρ_b. The scattering from a particle in solution is

$$I(s) = \langle |A_a(s) - \rho_s A_s(s) + \delta\rho_b A_b(s)|^2 \rangle_\Omega \qquad (3)$$

where $A_a(s)$ is the scattering amplitude from the particle in vacuo, $A_a(s)$ and $A_b(s)$ are, respectively, the scattering amplitudes from the excluded volume and the hydration layer, both with unitary density, $\delta\rho_b = \rho_b - \rho_s$, ρ_s is the density of the bulk solvent, and $\langle\ \rangle_\Omega$ denotes the orientational average in reciprocal space. Given the atomic coordinates, the program either predicts the solution scattering profile or fits the experimental data by adjusting the excluded volume of the particle and the contrast of the hydration layer $\delta\rho_b$.

For the rigid-body refinement of the position of the dimers in the atomic model of the yeast PDC, a dimer was oriented so that the 2-fold axis transforming it to the other dimer coincided with the Y axis, and its scattering amplitude was evaluated using Crysol. Any arbitrary configuration of the

Table 1: Comparison of the Molecular Masses Calculated from the Forward Scattering, Radii of Gyration, and Volume Fractions of Pyruvate Decarboxylases from Different Organisms at pH 6[a]

organism	molecular mass (kDa)	radius of gyration (nm)	volume fraction (%)	
			dimer	tetramer
Saccharomyces cerevisiae, brewer's yeast	226 ± 14	4.17 ± 0.06	0 ± 5	100 ± 5
Saccharomyces cerevisiae, recombinant *E. coli*	239 ± 19	3.95 ± 0.04	8.7 ± 2.6	91.3 ± 1.8
Pisum sativum cv. Miko, germinating seeds	500 ± 55	6.55 ± 0.1	nd[a]	nd
Zymomonas mobiliz, recombinant *E. coli*	245 ± 12	3.98 ± 0.06	8 ± 2	92 ± 3

[a] nd, not determined.

dimers in the tetramer can be obtained by moving the dimer away from the 2-fold axis, rotating it, and generating the symmetry-related one. The scattering amplitude of the latter and the intensity from the entire tetramer are rapidly calculated by shifting the dimer along the *Z* axis (*17*), thus allowing us to perform an automated search of the positional parameters providing the best fit to the experimental scattering curve from the tetramer.

RESULTS AND DISCUSSION

Integral Parameters of PDCs. Scattering measurements at pH values corresponding to the maximal catalytic activity (pH 6−6.5) provide a first characterization of the native structures. The molecular masses estimated from the forward scattering of the recombinant yeast enzyme and the bacterial enzyme in Table 1 correspond to a tetramer, as also calculated from the cDNA and measured by different analytical methods (native PAGE, gel filtration, and ultracentrifugation). The radii of gyration are, in general, somewhat lower than those obtained from solutions of the wild-type yeast enzyme, which tend to be more polydisperse. The only exception is the enzyme from germinating pea seeds. Gel filtration experiments indicate that the molecule elutes in the void volume and thus must have a molecular mass around 1 MDa (*14*). Electron microscopy suggests that the subunits form a tubular structure with varying lengths and diameters of 10−20 nm (Mücke, unpublished). The radius of gyration of the cross section (around 3 nm, Figure 1) and the mass per unit length from the SAXS patterns are consistent with a diameter of 8.4 nm, corresponding to 2 subunits/10 nm.

pH Dependence of the Quaternary Structure of the Recombinant Wild Type and Mutants E51Q, E51A, and G413W of PDC from Saccharomyces cerevisiae. SAXS data on brewer's yeast PDC (*1, 2*) indicate that the native tetramer at pH 6 progressively dissociates into dimers at higher pH values. Above pH 9, more than 70% of the enzyme is in the dimeric form. The cofactors TDP and Mg^{2+} stabilize the tetramers in the alkaline region. Although the brewer's yeast PDC is the one that has been studied most extensively, it is not yet precisely known which of the three known structural genes (PDC1, PDC5, or PDC6) is translated into protein. There are several isoforms (*29*) consisting of two different, α and β, subunits with a molecular mass of 59 and 61 kDa, respectively (*18*), but the dominant species is $\alpha_2\beta_2$. The α_4 form has been isolated and its crystal structure determined (*3, 4*). The amino acid sequence of the smaller subunit of brewer's yeast PDC corresponds to the structure of the PDC1 gene (Patzlaff, unpublished), and the recombinant enzyme described below is exclusively the product of this gene. It has kinetic and chemical properties that are very close to those of the wild-type yeast (*30*). The SAXS curves are also very similar and reveal a pH-dependent equilibrium between oligomers. There are, however, some differences in the radii of gyration and molecular mass estimates as a function of pH (Tables 1 and 2). The calculated molecular mass was about 230 kDa and thus corresponds to a tetramer for protein concentrations above 10 mg/mL, but this value drops to 180−200 kDa at concentrations between 3 and 5 mg/mL. This phenomenon was not observed during the measurements on brewer's yeast PDC (*1, 2*). At the catalytic optimum (pH 6), more than 90% of the recombinant wild-type enzyme are tetramers. However, the alkaline dissociation into dimers is almost complete at pH 9 (compared to 70% dimers for the brewer's yeast enzyme at the same pH). The estimated molecular masses and radii of gyration suggest that there is a further dissociation into monomers. The cofactors (TDP and Mg^{2+}) have no effect on the pH stability of the tetramers

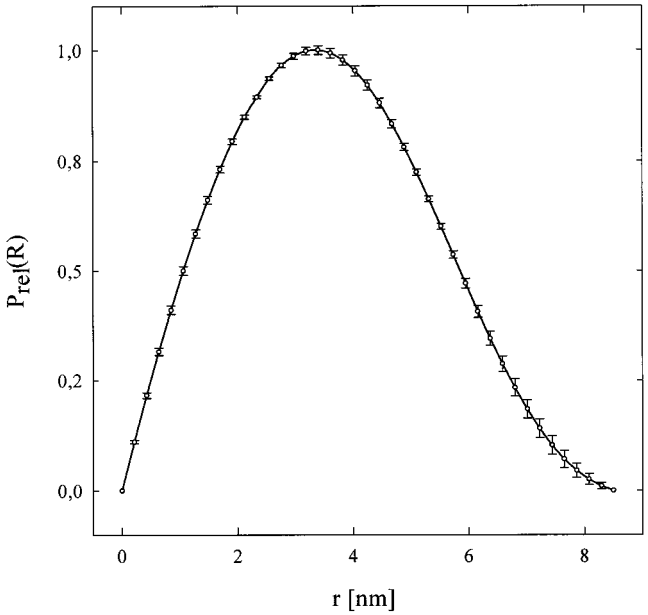

FIGURE 1: Distance distribution function of the cross section of PDC from germinating seeds of *Pisum sativum* at pH 6. The fit corresponds to a rodlike model.

Table 2: pH Dependence of the Forward Scattering (shown as molecular mass), Radius of Gyration, and Oligomer Content for the Recombinant Wild-Type of PDC from *Saccharomyces cerevisiae*

pH	molecular mass (kDa)	radius of gyration (nm)	volume fraction (%)	
			dimer	tetramer
6.1	214 ± 2.0	3.98 ± 0.04	8.7 ± 2.6	91.3 ± 1.8
6.5	210 ± 1.8	3.97 ± 0.05	6.1 ± 2.8	93.9 ± 1.8
7.2	190 ± 2.1	3.93 ± 0.04	7.7 ± 2.5	92.3 ± 1.7
7.8	152 ± 1.8	3.90 ± 0.04	36.7 ± 3.1	63.3 ± 2.1
8.3	95 ± 1.0	3.60 ± 0.05	86.0 ± 2.4	14.0 ± 1.6
8.9	96 ± 1.2	3.50 ± 0.06	97.3 ± 2.4	2.7 ± 1.6

(also in contrast to the brewer's yeast enzyme (*2*)); the scattering patterns of the recombinant yeast PDC in the presence and absence of cofactors are identical (not shown). These results are in good agreement with the molecular mass determination by gel filtration and kinetic experiments (*30*). The brewer's yeast enzyme is 5 times more stable than the homotetramer α_4 (*30*).

Analyses of the crystallographic model of native brewer's yeast PDC suggest that E51 is essential for cofactor binding and catalytic activity (*3*). Substitution of this amino acid by Q or A drastically lowers the substrate and cofactor binding affinities of the recombinant wild-type PDC of *S. cerevisiae* (*19*). Exchanging G413 by W completely prevents cofactor binding because of steric hindrance (Killenberg-Jabs, unpublished). Although only one amino acid is substituted, several differences were detected in the subunit interactions and influence of cofactors. E51Q has the highest similarity with wild type with regard to pH dependence of the radius of gyration and the apparent molecular mass obtained from the forward scattering. As expected from the kinetic studies on these species (*19*), the oligomer content at different pH values is also very similar. The two other mutants seem to be aggregated at pH 6—the optimum for catalytic activity. G413W does not bind cofactors and E51A binds them at a very low rate (*19*); both are catalytically completely inactive. These results are confirmed by our measurements: no really native tetrameric state of these mutants is found. Both mutants tend to aggregate at pH 6 and form higher oligomers than tetramers, although like all other yeast PDCs they still dissociate into dimers. The calculated oligomer content of the different mutants is in the same range as for the wild type. Higher pH values result in a complete dissociation of the PDCs into dimers. At these alkaline pH values, the cofactors do not influence the dimer/tetramer ratio for G413W and E51A, but they stabilize the native tetrameric structure of E51Q. The SAXS results obtained with PDC mutants suggest that amino acid substitutions which strongly affect the catalytic activity and cofactor binding of PDC from *S. cerevisiae* also lead to changes in the quaternary structure of the enzyme. The lower the affinity for the cofactor, the more unspecific aggregation of tetramers occurs at the pH corresponding to the optimum catalytic activity of the wild-type enzyme.

Shape Estimation of the Recombinant Wild Type of PDC from Saccharomyces cerevisiae and Comparison with the Crystallographic Model. The shape of the native tetrameric PDC from recombinant wild type from *S. cerevisiae* at a resolution of 2.3 nm was evaluated ab initio from its solution-scattering curve, yielding a fit with $\chi = 0.86$ (Figure 2). Standard deviations are plotted; it is seen that the fits are within the error limits and $\chi < 1$. The corresponding envelope in Figure 3 coincides well with the shape of the tetrameric yeast PDC found earlier (*2*). Figure 5 illustrates its comparison with the crystallographic model (*4*) of the brewer's yeast PDC (PDB entry 1pvd). The envelope obtained from solution scattering yields a fair description of the gross structure of the enzyme, whereas finer details are lost because of the limited resolution. The major difference in the quaternary structure of the two models is that the dimers in the crystallographic model are parallel to each other, whereas in our model they are tilted, as already reported earlier (*2*). The theoretical scattering was evaluated

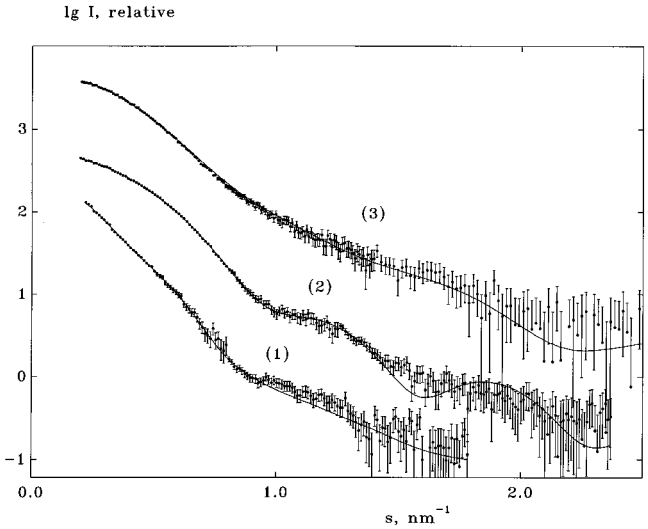

FIGURE 2: Solution scattering curves of PDC from *Pisum sativum* (1), *Zymomonas mobilis* (2), and *Saccharomyces cerevisiae* (3). Dots with error bars, experimental data; solid lines, scattering from the restored shapes in Figure 3.

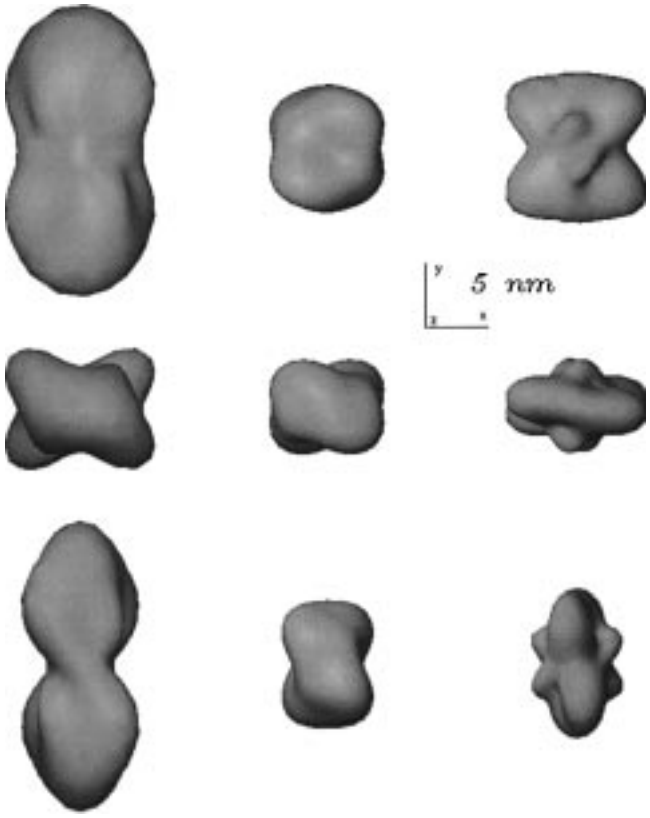

FIGURE 3: Low-resolution envelopes of PDC from *Pisum sativum* (left), *Zymomonas mobilis* (middle), and *Saccharomyces cerevisiae* (right) restored from solution scattering data. Axes correspond to the orientation in the middle row; top row, rotated counterclockwise around *X* by 90°; bottom row, the same rotation followed by a counterclockwise rotation of 90° around *Y*.

from the crystallographic model (*4*) using the program Crysol (*28*). The comparison of the calculated curve with the experimental data in Figure 4 revealed noticeable systematic deviations in the region of the first shoulder, indicating that the quaternary structure of the tetramer in solution may be different from that in the crystal—such a difference has recently been observed for aspartate transcarbamylase (*31*). As the ab initio shape determination suggests that the two

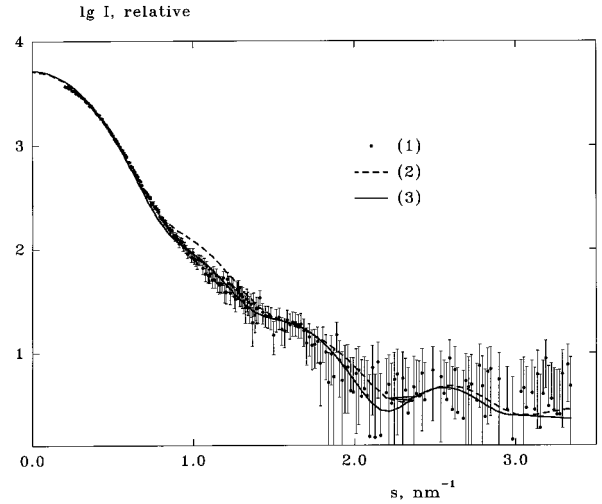

FIGURE 4: Experimental scattering from the recombinant wild type of PDC from *Saccharomyces cerevisiae* (1), calculated scattering from the crystallographic model of brewer's yeast α_4 form PDC (2), and the scattering from the model obtained by the rigid-body refinement (3).

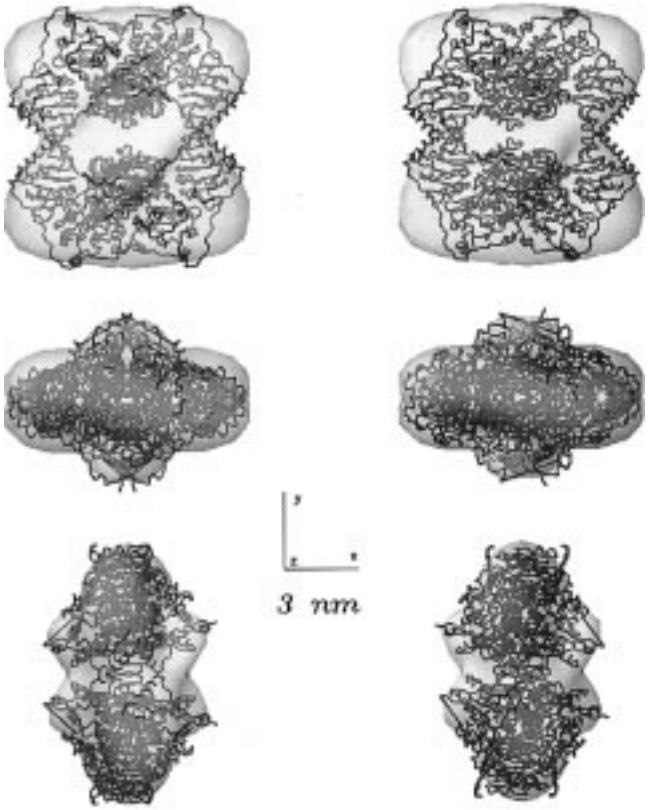

FIGURE 5: Low-resolution model of the yeast PDC (transparent envelopes) merged with the crystallographic model (4) (left) and with the model obtained by the rigid-body refinement (right). The orientation of the models is the same as in Figure 3.

dimers are tilted, rigid-body modeling of the structure of the tetramer in solution was performed as described in the Materials and Methods section. In keeping with the low resolution of the data, only two parameters were varied, the distance between the centers of mass of the dimers along the *Z* axis in the orientation in Figure 5, middle row, and the tilting angle between them (opposite rotation around the *Z* axis). The solution providing the best fit shown in Figure 5 corresponds to a tilting angle of 10° and a distance between the dimers of 5.1 nm (i.e., 0.4 nm lower than in the crystal structure), which yields the rms displacement of 0.22 nm between the atomic positions in the two structures. The discrepancy with the experimental data drops from $\chi = 1.87$ for the crystal structure to 1.23 for the solution model. As seen from Figure 5, the tilting angle between the dimers resulting from the rigid-body modeling is close to that in the envelope restored ab initio. A similar movement of the dimers and a resulting asymmetry of the tetramer were found in the crystallographic structure of the activated brewer's yeast PDC (*12*).

pH Dependence of the Quaternary Structure and Shape Estimation of PDC from Germinating Seeds of Pisum sativum. As already mentioned, PDCs from plant seeds (e.g., maize, beans, wheat) have generally more complex oligomeric structures. Interestingly though, the values of the kinetic parameters such as substrate affinity, catalytic activity, and reconstitution rate with the cofactors are close to those of the yeast enzyme (*10*, *14*, *15*). Recent studies of enzyme activation and thiol group modifications have, however, revealed significant quantitative differences (*10*), and the SAXS experiments were aimed at correlating these with possible structural differences. The more complex structure of the plant enzymes considerably complicates the preparations and interpretation of the scattering patterns. The preparative yields for pea PDC are very low, and subsequent concentration steps lead to aggregation. The resulting solutions tend to be very polydisperse (*14*, *32*). Modified preparative conditions and new protein concentration techniques (*10*) resulted in monodisperse solutions, yielding interpretable scattering patterns. The best fitting results were obtained with a rodlike system (Figure 1). At pH values between catalysis and stability optimum (around pH 6) and the beginning of cofactor dissociation (above pH 7.5), the molecule seems to be a cylindrical stack of dimers or tetramers with a diameter of 8.4 nm and 2 units/10 nm. Transmission electron microscopy of negatively stained pea PDC samples also indicates that the enzyme has a rodlike structure (Mücke, unpublished). Above pH 9, this complex structure breaks down into smaller entities with R_G values compatible with tetramers (Figure 6A). The plant PDC seems to be a compact dimer of dimers at pH 9, like the yeast enzyme at pH 6. The cofactors stabilize the octameric structure even at this high pH value. Below pH 6, aggregation already occurs during the measurement period of 10−20 min. According to the molecular mass estimates, PDC from pea seeds forms octamers at pH 6. The shape of this assembly was evaluated from the corresponding experimental curve as described in the Materials and Methods section. The resulting fit to the experimental curve ($\chi = 0.92$) is presented in Figure 2, and the restored shape at a resolution of 3.8 nm is displayed in Figure 3. As seen from this figure, the tetramer of the pea enzyme is similar to that from yeast and bacteria, whereas the octamer is formed by side-by-side arrangement of the tetramers, leading to a rather elongated assembly.

pH Dependence of the Quaternary Structure and Shape Estimation of PDC from Zymomonas mobilis. Despite the same oligomeric structure, PDC from *Z. mobilis* differs in its kinetic properties from all other ones. It is not activated by its substrate pyruvate (resulting in a hyperbolic *v*/*S* plot) but reaches twice the value for the catalytic activity (180 U/mg compared to 60−80 U/mg for the other species (*13*)). The cofactors are tightly but not covalently bound. Gel

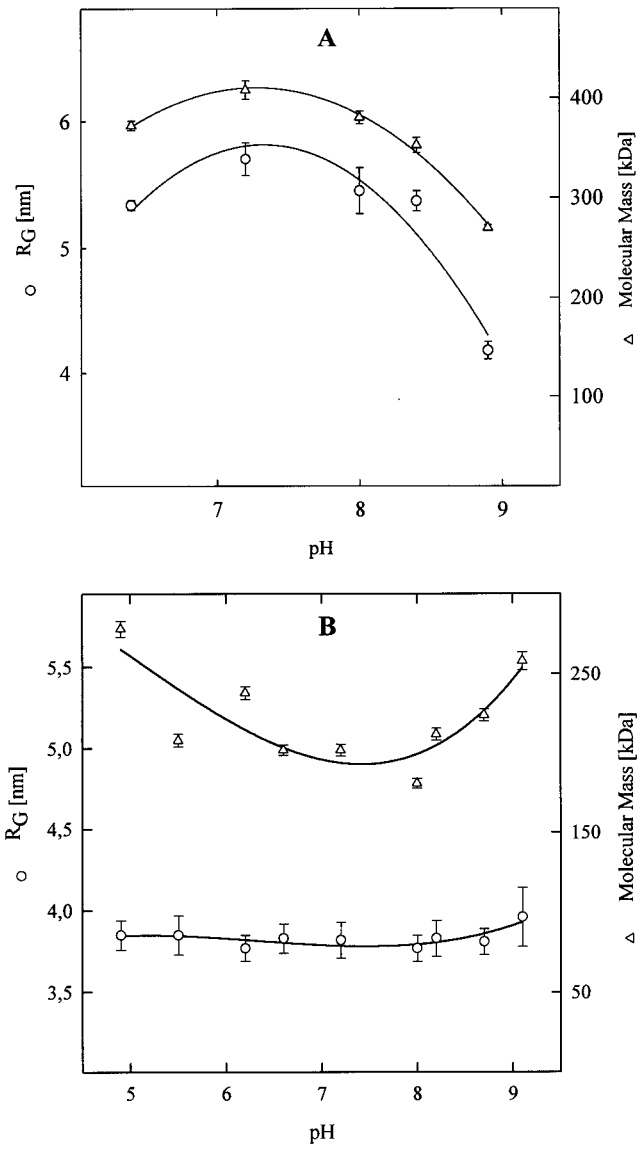

FIGURE 6: pH dependence of the forward scattering (expressed as molecular mass) and radius of gyration of PDC from germinating seeds of *Pisum sativum* (A) and from the bacterium *Zymomonas mobiliz* (B).

filtration experiments indicate a tetrameric structure even for the cofactor-free apoenzyme (*33*). The analysis of scattering patterns as a function of pH confirms these results. If there exists a pH-dependent oligomer equilibrium, the calculated volume fraction of dimers is always below 18%—even under extreme alkaline conditions. The lowest values for R_G and molecular mass were obtained at pH 8 (Figure 6B), where the preparation of apoenzyme of this PDC species is usually done via dialysis (*33*). Either the cofactors are bound in a completely different way in PDC from *Z. mobilis* without need of subunit dissociation or binding is very rapid and already completed during the incubation times used in our experiments (10−15 min). Low-resolution shape determination of the PDC from *Z. mobilis* yields $\chi = 0.92$ (Figure 2). The restored shape of the tetramer of the bacterial PDC in Figure 3 at a resolution of 2.3 nm appears to be more compact than the yeast enzyme and displays a more pronounced contact region between the dimers, which may explain the high stability of the tetrameric structure of PDC from *Z. mobilis*.

ACKNOWLEDGMENT

We thank Arndt Dietrich, Margrit Killenberg-Jabs, and Jörg Schäffner for the preparation of the enzymes.

REFERENCES

1. König, S., Svergun, D., Koch, M. H. J., Hübner, G., and Schellenberger, A. (1992) *Biochemistry 31*, 8726−8731.
2. König, S., Svergun, D., Koch, M. H. J., Hübner, G., and Schellenberger, A. (1993) *Eur. Biophys. J. 22*, 185−194.
3. Dyda, F., Furey, W., Swaminathan, S., Sax, M., Farrenkopf, B., and Jordan, F. (1993) *Biochemistry 32*, 6165−6170.
4. Arjunan, P., Umland, T., Dyda, F., Swaminathan, S., Furey, W., Sax, M., Farrenkopf, B., Gao, Y., Zhang, D., and Jordan, F. (1996) *J. Mol. Biol. 256*, 590−600.
5. Muller, Y. A., Lindqvist, Y., Furey, W., Schulz, G. E., Jordan, F., and Schneider, G. (1993) *Structure 1*, 95−103.
6. Pletcher, J., and Sax, M. J. (1972) *J. Am. Chem. Soc. 94*, 3998−4005.
7. Schellenberger, A. (1967) *Angew. Chem. 79*, 1050−1061.
8. Gounaris, A. D., Turkenkopf, I., Buckwald, S., and Young, A. (1971) *J. Biol. Chem. 246*, 1302−1307.
9. Hübner, G., Weidhase, R., and Schellenberger, A. (1978) *Eur. J. Biochem. 92*, 175−181.
10. Dietrich, A., and König, S. (1997) *FEBS Lett. 400*, 42−44.
11. König, S., Hübner, G., and Schellenberger, A. (1990) *Biomed. Biochim. Acta 49*, 465−471.
12. Lu, G., Dobritzsch, D., König, S., and Schneider, G. (1997) *FEBS Lett. 403*, 249−253.
13. Bräu, B., and Sahm, H. (1986) *Arch. Microbiol. 144*, 296−301.
14. Mücke, U., König, S., and Hübner, G. (1995) *Biol. Chem. Hoppe-S. 376*, 111−117.
15. Mücke, U., Wohlfahrt, T., Fiedler, U., Bäumlein, H., Rücknagel, K. P., and König, S. (1996) *Eur. J. Biochem. 237*, 373−382.
16. Svergun, D. I., Volkov, V. V., Kozin, M. B., and Stuhrmann, H. B. (1996) *Acta Crystallogr. A52*, 419−426.
17. Svergun, D. I., Volkov, V. V., Kozin, M. B., Stuhrmann, H. B., Barberato, C., and Koch, M. H. J. (1997) *J. Appl. Crystallogr. 30*, 798−802.
18. Sieber, M., König, S., Hübner, G., and Schellenberger, A. (1983) *Biomed. Biochim. Acta 42*, 343−349.
19. Killenberg-Jabs, M., König, S., Eberhardt, I., Hohmann, S., and Hübner, G. (1997) *Biochemistry 36*, 1900−1905.
20. Koch, M. H. J., and Bordas, J. (1983) *Nucl. Instrum. Methods 208*, 461−469.
21. Boulin, C., Kempf, R., Koch, M. H. J., and McLaughlin, S. M. (1986) *Nucl. Instrum. Methods A249*, 399−407.
22. Boulin, C. J., Kempf, R., Gabriel, A., and Koch, M. H. J. (1988) *Nucl. Instrum. Methods A269*, 312−320.
23. Gabriel, A., and Dauvergne, F. (1982) *Nucl. Instrum. Methods 201*, 223−224.
24. Svergun, D. I., Semenyuk, A. V., and Feigin, L. A. (1988) *Acta Crystallogr. A44*, 244−250.
25. Svergun, D. I. (1991) *J. Appl. Crystallogr. 24*, 485−492.
26. Svergun, D. I. (1992) *J. Appl. Crystallogr. 25*, 495−503.
27. Svergun, D. I., and Stuhrmann, H. B. (1991) *Acta Crystallogr. A47*, 736−744.
28. Svergun, D. I., Barberato, C., and Koch, M. H. J. (1995) *J. Appl. Crystallogr. 28*, 768−773.
29. Farrenkopf, B. C., and Jordan, F. (1992) *Prot. Expr. Purif. 3*, 101−107.
30. Killenberg-Jabs, M., König, S., Hohmann, S., and Hübner, G. (1996) *Biol. Chem. Hoppe-S. 377*, 313−317.
31. Svergun, D. I., Barberato, C., Koch, M. H. J., Fetler, L., and Vachette, P. (1997) *Proteins 27*, 110−117.
32. Mücke, U., König, S., and Koch, M. H. J. (1994) *Hasylab Jahresbericht* 1994, 809−810.
33. Diefenbach, R. J., and Duggleby, R. G. (1991) *Biochem. J. 276*, 439−445.

BI972125V